

Optimisation of a High Speed Copper Rotor Induction Motor for a Traction Application

Nicolas Rivière
Motor Design Limited
Wrexham, UK

nicolas.riviere@motor-design.com

Marco Villani
University of L'Aquila
L'Aquila, Italy

marco.villani@univaq.it

Mircea Popescu
Motor Design Limited
Wrexham, UK

mircea.popescu@motor-design.com

Abstract—This paper deals with the optimisation of a 200kW, 20krpm machine for an electric vehicle application using Motor-CAD and optiSLang software. The main goal of the research is to design a low cost, rare-earth free magnet motor while ensuring mass production feasibility and providing higher performance than current available technologies. The induction motor with copper rotor cage, either die-casted or fabricated, is selected as a potential candidate. The stator winding is of hairpin type and both rotor and stator parts benefit from direct cooling. The machine is optimised electromagnetically and thermally to meet the peak and continuous performance requirements with respect to the project specifications. In particular, the efficiency computation over the typical WLTP3 drive cycle is considered in the optimisation process. The latter is looked into details and uses a meta-model based approach which allows to evaluate thousands of design topologies in a computationally efficient way for a given optimisation scenario.

Keywords— High speed, induction motor, optimisation, meta-models, hairpin winding, rotor die-casting.

I. INTRODUCTION

The society has been witnessing a significant shift in the transportation industry over the last decade to support the transition to a climate-resilient, energy-efficient and low-carbon economy [1]. Despite a notable growth of the Electric Vehicles' (EVs) market [2], car manufacturers continue to face new challenges in order to substantially reduce greenhouse gases and break dependency on fossil fuels, while maintaining high levels of efficiencies.

Most of passenger EVs sold in recent years are using Permanent Magnet (PM) traction motors with neodymium-based material in the rotor [3], since they inherently lead to more compact systems with higher overall performance in terms of efficiency, power and torque density. However, after the dramatic surge of rare-earth materials' price in 2011, motor designers are intensively investigating viable alternatives to PM technologies that would provide comparable performances. The copper rotor Induction Machine (IM) is therefore considered as a potential candidate.

In various studies, it was illustrated how the IM compared to PM motors [4, 5]. It was found that to deliver similar performance, the IM requires bigger dimensions and higher current ratings. Despite this, the technology is well established in the automotive industry (e.g Tesla 60S, Audi e-tron) as a PM-free motor and still represents an attractive and feasible solution for future EVs. The IM benefits from a simple structure, is robust and versatile, and presents cost-effective manufacturing aspects and fault tolerant capability [5].

The present study focuses on the optimisation of a high-speed copper rotor IM for the next generation electric powertrains, ensuring the industrial feasibility for mass production with low manufacturing costs. The main project requirements are reported in Table I. The Key Performance

Indicators (KPIs), including efficiency, specific torque, specific power and power density are defined based on the Tesla 60S electrical machine [6, 7].

Additional boundary conditions are set based on the vehicle requirements, considering the Jaguar XJMY21 as a target. The machine is cooled by a conventional housing Water Jacket (WJ) combined in parallel with a shaft cooling system (as per references [8, 9]), using a mixture of ethylene, glycol and water as a coolant.

TABLE I. MOTOR REQUIREMENTS

Parameter	Unit	Value	Comment
Specific power	kW/kg	≥ 4.3	Peak value, 30% increase based on Tesla 60S (active parts only)
Specific torque	Nm/kg	≥ 8.2	Peak value, 30% increase based on Tesla 60S (active parts only)
Power density	kW/l	≥ 8	Peak, active volume only
Maximum speed	krpm	20	-
Peak power	kW	200	30s, up to base speed (≈ 5200 rpm)
Peak torque	Nm	370	Up to base speed
Continuous torque	Nm	152	@ Low speed (≈ 2000 rpm)
Continuous power	kW	70	@ Maximum speed
Efficiency	%	≥ 96	Peak value, 3% increase based on Tesla 60S (93%)
		≥ 94.5	Over WLTP3 drive cycle
Phase current	A_{rms}	≤ 500	@720Vdc
Machine length	mm	≤ 310	Including bearings
Housing diameter	mm	≤ 250	-
Flow rate	l/min	≤ 10	Shared between the shaft and the housing cooling systems
Pressure drop	kPa	≤ 20	Housing WJ only
Fluid outlet temperature	$^{\circ}C$	≤ 90	-
Ambient temperature	$^{\circ}C$	50	-
Rotor cage temperature	$^{\circ}C$	≤ 180	Limited by the bearings' thermal capability
Winding temperature	$^{\circ}C$	≤ 180	Limited by the winding insulation (class H)

II. PRELIMINARY DESIGN

A complete design procedure is essential to validate the specifications before committing to make any physical prototype [10]. The logic behind the design process is outlined in Fig. 1. The first task consists in finding an initial design based on the main requirements such as torque, power, maximum speed and available space.

During this stage, design choices are taken in order to properly chose fundamental parameters such as the slot/pole/bar combination, the optimal winding pattern, the main dimensions and the active materials. The obtained design is then used as a starting point for further optimisation. The electromagnetic, thermal and mechanical constraints are considered throughout the whole machine design process.

A. Active geometry

The axial and radial geometry cross sections of the initial active design obtained after phase 2 are shown in Fig. 2 and Fig. 3, respectively. Main parameters are summarized in Table II. The 4 poles, 36 slots, 50 bars topology appeared to be the most recommended combination for further optimisation [11, 12]. For mechanical reasons, the rotor slots are closed. Also note that the active dimensions comply with the maximum package envelope.

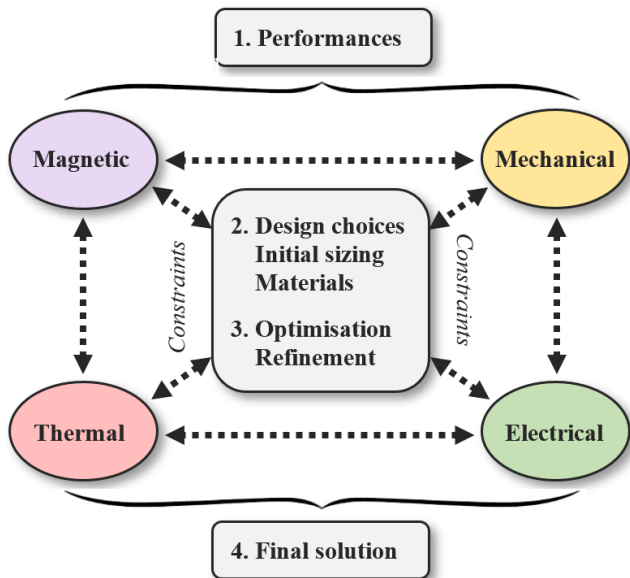


Fig. 1. Example of design procedure

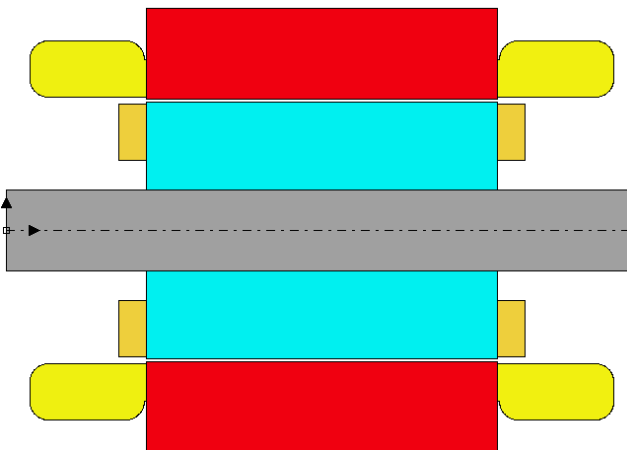


Fig. 2. Axial machine geometry section of the initial design

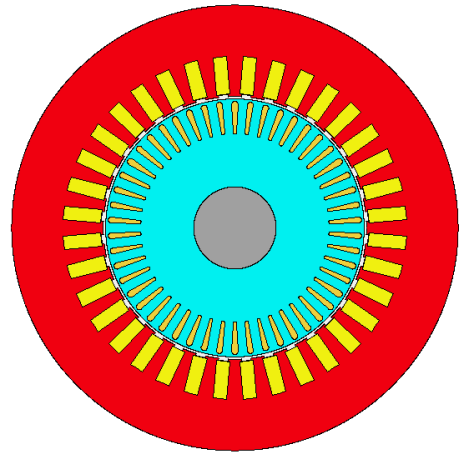


Fig. 3. Radial machine geometry section of the initial design

TABLE II. MAIN MACHINE DIMENSIONS

Parameter	Unit	Value
Stator slots	-	36
Pole pairs	-	2
Rotor bars	-	50
Stator outer diameter	mm	190
Rotor outer diameter	mm	110
Airgap length	mm	1
Active length	mm	150
Active weight	kg	36

B. Stator winding

The proposed design makes use of the great performance of the proprietary hairpin stator winding, that is composed of preformed hairpin like shape sections of rectangular profile conductors. This technology suits well distributive windings and leads to repeatable manufacturing and robust construction at the critical connection between conductors [13].

The winding layout is shown in Fig. 4. A double layer pattern with four conductors per slot is selected to ensure production feasibility. The three phases are star-connected and present coils in series to meet the inverter requirements. The rectangular stator slots provide a snug fit for the conductors in order to reach a high slot fill factor (0.73).

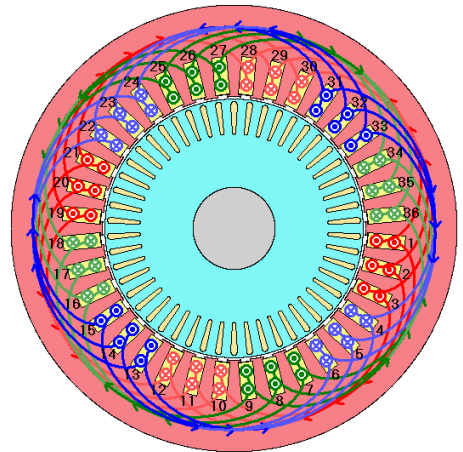


Fig. 4. Winding pattern and slot conductors distribution

C. Materials

Materials' selection for the IM includes electrical steel and copper alloys. In order to meet the KPIs along with the cost restrictions, materials with the best compromise between cost and performance have been selected: M235-35A silicon iron steel, fully-process, 0.35mm thick, for the rotor and stator cores; CuAG0.04 and Cu-ETP copper alloys for the fabricated and die-casted rotor cages, respectively.

D. Performances

The peak performance over the full speed range of the machine are calculated using Motor-CAD software with a Maximum Torque per Ampere (MTPA) control strategy and considering the electrical limits specified in the introduction. The efficiency maps are given in Fig. 5. The peak power/torque/efficiency targets are fulfilled, together with the KPIs, based on the active weight and dimensions given in Table II.

The WLTP3 drive cycle is considered to evaluate the machine energy consumption (Fig. 6). The torque-speed demand on the motor side is defined based on a vehicle model implemented into Motor-CAD, using the Jaguar XJMY21 data. The efficiency calculated over the WLTP3 drive cycle is around 93.3%, which is less than the required value. This parameter is therefore included in the objective function of the optimisation problem presented hereinafter.

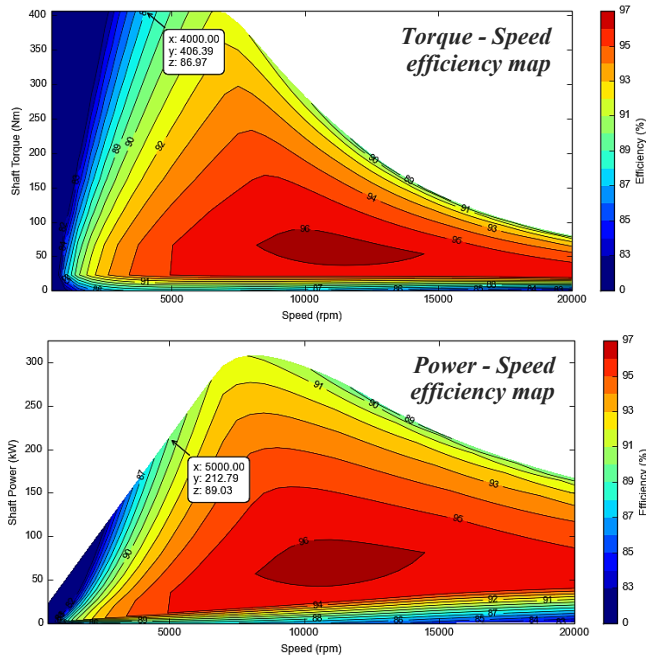


Fig. 5. Efficiency maps of the initial design

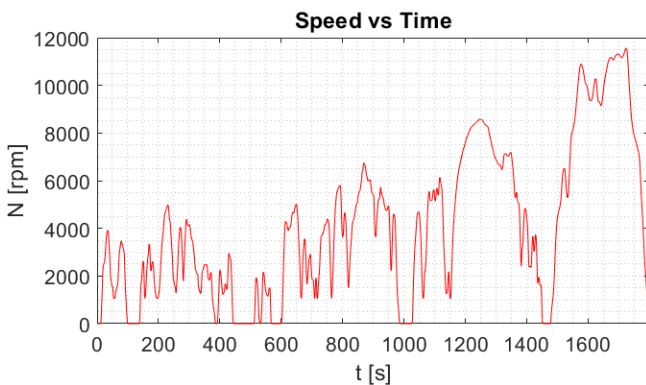


Fig. 6. WLTP3 drive cycle

III. OPTIMISATION

An optimisation procedure has been set up using optiSLang and Motor-CAD software. Motor-CAD is driven by optiSLang from customized Python scripts in order to define, control and extract parameters of interest. A possible optimisation workflow is presented in Fig. 7. After the definition of the design variables and model responses, a sensitivity analysis is performed. The design space is scanned by sampling methods and for each design the model responses are determined. Then the optiSLang solver calculates the best approximation model for each response, also called “Meta-model of Optimal Prognosis” (MOP). An optimisation is finally performed directly on the MOP. The strengths of this strategy are the following:

- it gives an insight of where to concentrate the efforts for given motor requirements;
- thousands of designs can be evaluated within minutes by the optimiser, either local or global, and for different set of objectives and constraints;
- the machine can be optimised across its full operating range, including both magnetic and thermal performance.

A two-stages optimisation has been implemented using this approach. The machine introduced in section II is initially optimised electromagnetically, in order to find the best compromise between active weight and efficiency over the WLTP3 drive cycle. The obtained design is then thermally optimised to meet the continuous performance requirements.

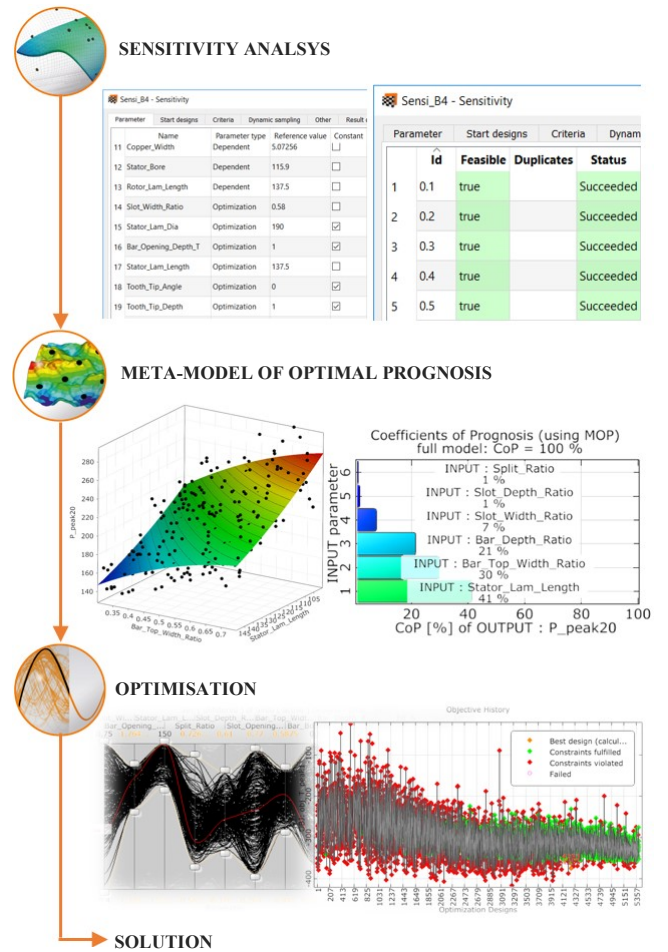


Fig. 7. Optimisation workflow using optiSLang

A. Electromagnetic optimisation

The optimisation problem is non-linear and multi-objective, as formulated below:

$$\begin{aligned} & \min (\text{Active length}) \ \& \ \max (\text{Efficiency over WLTP3}) \\ & \text{s.t. Peak power @ Base speed} \geq 200 \text{ kW} \\ & \text{s.t. Active weight} \leq 44.6 \text{ kg} \end{aligned}$$

To reduce the computational time in Motor-CAD, the efficiency is calculated from five characteristic operating points, determined beforehand using a clustering function. The method consists in grouping points into “clusters”, each of them being characterized by a centroid and weight, as shown in Fig. 8. The weighted average value of the efficiency is then used in the objective function.

The variables with their ranges are reported in Table III. Using ratios of geometric parameters allows to avoid failed designs in Motor-CAD due to potential intersecting lines in the geometry. This point is crucial since the accuracy of the MOP-based optimisation is directly affected by the number of succeeded designs generated from the sensitivity analysis. The ratios used as variables are detailed below:

- **Split ratio** = Stator inner diameter / Stator outer diameter
- **Slot depth ratio** = Slot depth / (Slot depth + Stator yoke)
- **Slot width ratio** = Slot width / Slot pitch
- **Bar depth ratio** = Bar depth / (Bar depth + Rotor yoke)
- **Bottom bar width ratio** = Bottom bar width / Bar pitch
- **Top bar width ratio** = Top bar width / Bar pitch.

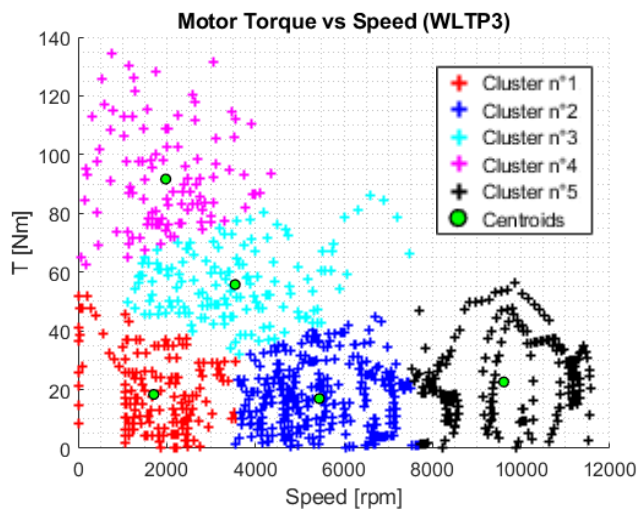


Fig. 8. Operation points grouped in clusters (motor mode only)

TABLE III. MACHINE DIMENSIONS RANGE

Variable	Min	Max	Unit
Airgap length	0.8	1.5	mm
Active length	100	175	mm
Bar opening depth	0.5	2	mm
Split ratio	0.5	0.7	-
Slot depth ratio	0.3	0.6	-
Bar depth ratio	0.2	0.8	-
Slot width ratio	0.4	0.7	-
Bottom bar width ratio	0.3	0.6	-
Top bar width ratio	0.3	0.6	-

A sensitivity analysis is performed using the Advanced Latin Hypercube Sampling approach with 400 samples. The simulation completed in approximately 24 hours, since each design in Motor-CAD requires between 3 and 4 minutes, from parameter assignment to responses’ extraction. The plot provided in Fig. 9 gives an overview of the MOP results, where the Coefficients of Prognosis (CoPs) are independent measures defined with the aim of assessing the quality of the proposed models.

In fact, CoPs indicate how much input parameters and responses interact with each other. As a result, from the CoP matrix the most important input parameters can be determined with respect to each response and the forecast quality of the identified surrogate model can be evaluated. In Fig. 9, the last column contains the full model CoPs for every output parameter while the single CoP values of the input parameters are shown in lines. For visibility reason, only CoPs of the stator parameters are reported.

The active length and the slot depth ratio parameters have therefore a major impact on the design performance. For illustration, the MOP for the peak power at base speed is plotted with regards to these two parameters (Fig. 10). The predicted variations validate well the first line of the CoP matrix. Note that the total CoP values could be improved further by additional sampling data. However, such high values usually provide sufficient confidence in the models to be used for optimisation.

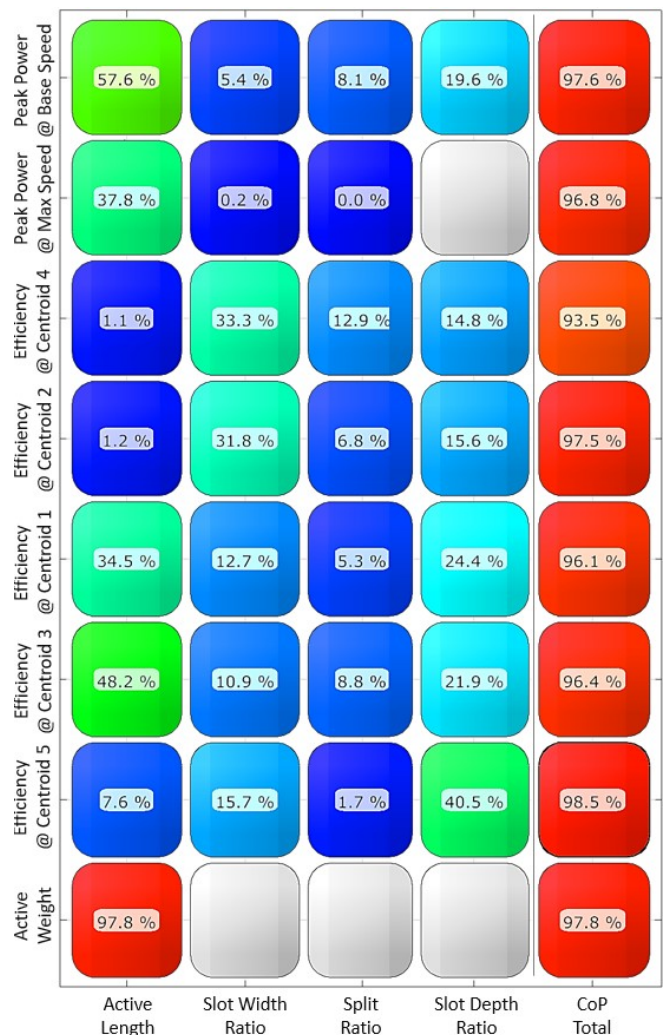


Fig. 9. CoP matrix with stator parameters only

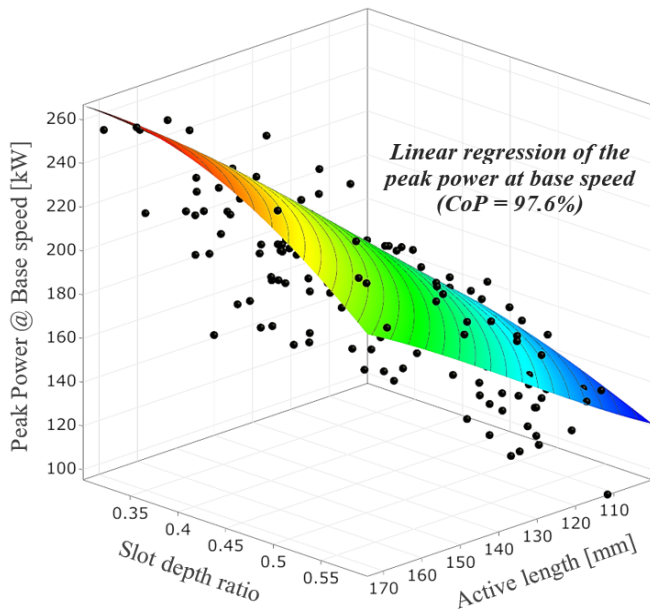


Fig. 10. MOP for the peak power at base speed

A global optimisation was performed on the MOP. More than 10000 designs were analysed within minutes. The resulting Pareto frontier of the multi-objectives evolutionary algorithm is shown in Fig. 11. There is a clear trade-off between the machine's size and energy consumption. The design number 10227, highlighted in blue, is selected for the next optimisation phase. The active length and efficiency of the selected design are 161mm and 95.1%, respectively. The efficiency is now higher than the required value.

The radial geometry sections of the initial and optimal designs are compared in Fig. 12. In addition to being longer, the selected topology presents a higher split ratio, bigger rotor bars and wider stator slots. Peak performance are calculated in Motor-CAD with the optimal set of variables. The results reported in Fig. 13 match perfectly the peak performance requirements and show a wide operating zone at peak efficiency (96%). The efficiency calculated over the WLTP3 drive cycle in motoring mode reached 95.05, which is very close to the MOP value.

Objective Pareto Plot

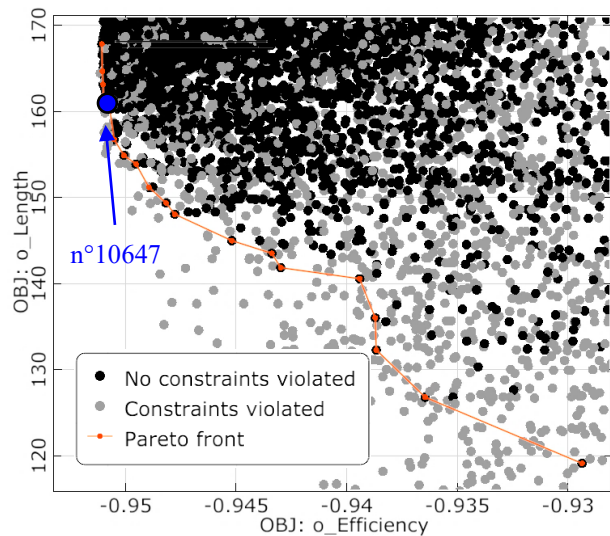


Fig. 11. Pareto front: Active length vs Efficiency

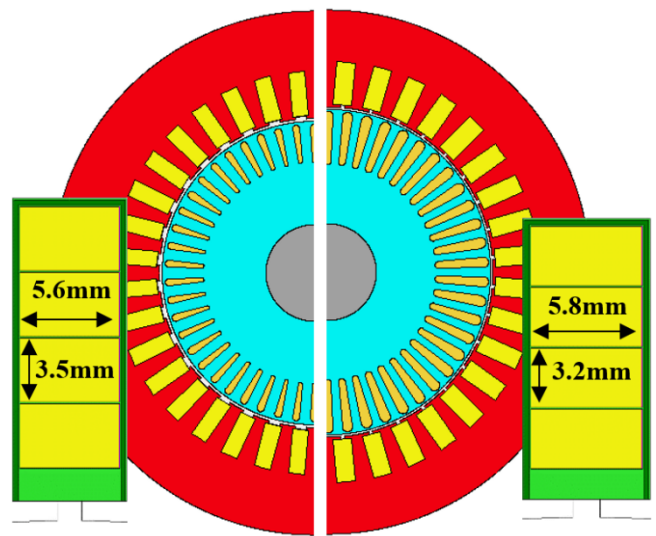


Fig. 12. Radial machine geometry sections (left: reference; right: optimum)

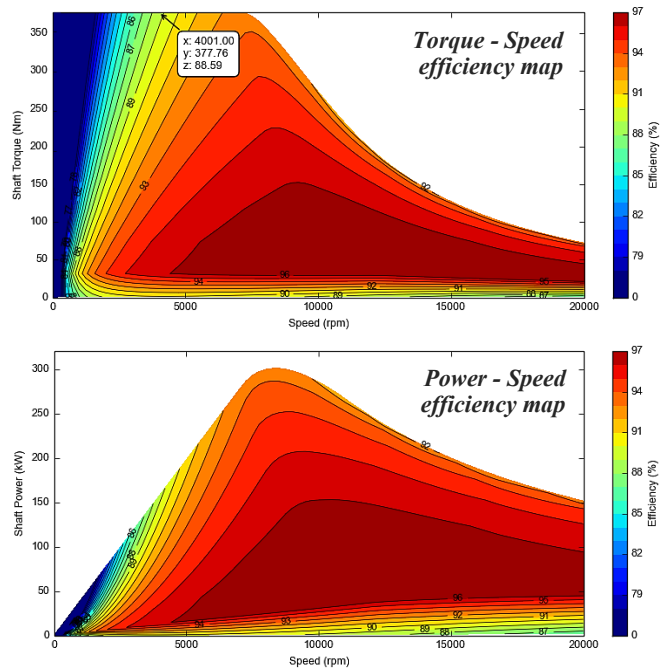


Fig. 13. Performance maps of the optimal design

Must be said, the efficiency over the complete drive cycle, considering both motoring and generating modes, is about 94.8%. The clustering method could be extended to the complete cycle. However, the present design still meets the requirements, thence it is selected for further analysis.

B. Thermal optimisation

The design selected in last section was optimised thermally with a similar MOP-based approach. The variables include the housing thickness, the channel dimensions for the WJ and shaft cooling systems, and the flow rate distribution between the two cooling paths.

The final machine's package envelope fits into the maximum available space, as shown in Fig. 14. The main cooling system characteristics are reported in Table IV, and the continuous performances, validated in Motor-CAD, are given in Fig. 15. The low-speed torque and high-speed power requirements are met.

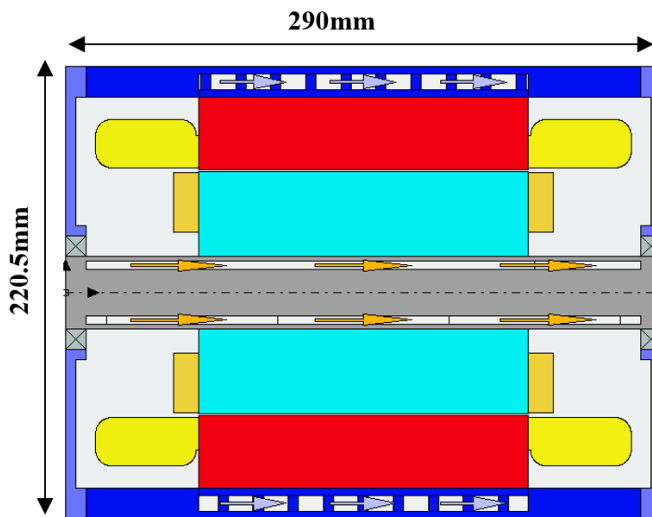


Fig. 14. Axial machine geometry section of the final design

TABLE IV. MAIN CHARACTERISTICS OF THE COOLING SYSTEM

Parameter	WJ	Shaft	Unit
Fluid inlet temperature	75	75	°C
Fluid outlet temperature	83.38	79.26	°C
Fluid flow rate	5.75	4.25	l/min
Pressure drop	10.42	-	kPa
Channel number	10	1	-
Channel width	12	-	mm
Channel height	8	4	mm

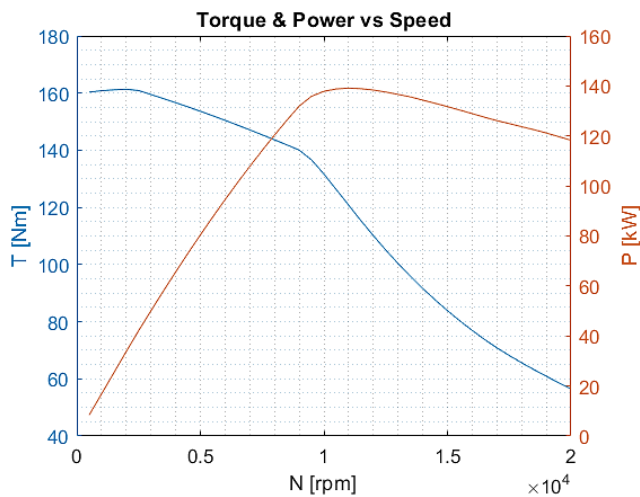


Fig. 15. Continuous performance of the final design

IV. CONCLUSION

This paper has presented the optimisation of a high-speed copper rotor induction motor for an electrical vehicle application using Motor-CAD and optiSLang software. The main project requirements are mass production feasibility, low cost and high performance.

A meta-model based approach has been proposed to optimise the machine, electromagnetically first, then thermally. The quality of the optimal design has been

validated with Motor-CAD, in order to demonstrate the effectiveness of the method.

In particular, the optimized solution obtained using the meta-models approach provides higher efficiency, higher specific torque and higher specific power levels compared with the Tesla 60S motor baseline.

ACKNOWLEDGMENT

This project has received funding from the European Union's Horizon 2020 Research and Innovation Programme under the Grant Agreement No 770143.

REFERENCES

- [1] "The roadmap for transforming the EU into a competitive, low-carbon economy by 2050", European Commission Climate Action.
- [2] "Electric vehicles will grow from 3 million to 125 millions by 2030, International Energy Agency forecasts", CNBC, 2018.
- [3] "93% of Evs sold in 2018 used permanent magnet traction motors", Charged Electrical Vehicle Magazine, 2019.
- [4] M. Burwell, J. Goss and M. Popescu, "Performance/Cost comparison of the induction motor and permanent magnet motor in a hybrid electric car", TechnoFrontier, Tokyo, Japan, 2013.
- [5] D. Fulton, C. Mi, Z-Q. Zhu, W. Cai, "Panel discussion on motors: permanent magnet, induction, switched reluctance", SAE Powertrain Electric Motors Symposium, Shanghai, 2011.
- [6] "Tesla is upgrading Model S/X with new, more efficient electric motors", Electrek, 2019.
- [7] K-C. Kim, "Driving characteristic analysis of traction motors for electric vehicle by using FEM", Ansys Users Conference, Seoul, Korea, 2014.
- [8] "A detailed look into the Audi E-Tron EV", Carlist.my, 2018.
- [9] L. Fedoseyev and E-M. Pierce Jr, "Rotor assembly with heat pipe cooling system", US patent application # 2014/0368064 A1.
- [10] M. Rosu, P. Zhou, D. Lin, D. Ionel, M. Popescu, F. Blaabjerg, V. Rallabandi, D. Staton, "Multiphysics simulation by design for electrical machines, power electronics, and drives", IEEE Press, Wiley, New-York, 2018.
- [11] R. Richter, "Electrical machines: induction machines (Elektrische Maschinen: Die Induktionsmaschinen)", Vol. IV, 2nd edn, Birkh"user Verlag, Basle and Stuttgart, 1954.
- [12] B. Heller and V. Hamata, "Harmonic Field Effects in Induction Machines", Elsevier Scientific, Amsterdam, 1977.
- [13] "Inside the HVH hybrid motor – Technical insights on Remy's "off-the-shelf" hybrid motor solutions", White Paper, Remy Electric Motors, 2009.